



ELSEVIER

Available online at [www.sciencedirect.com](http://www.sciencedirect.com)

SCIENCE @ DIRECT®

Nuclear Physics B (Proc. Suppl.) 141 (2005) 244–249

NUCLEAR PHYSICS B  
PROCEEDINGS  
SUPPLEMENTS

[www.elsevierphysics.com](http://www.elsevierphysics.com)

## Quark–gluon vertex in arbitrary kinematics\*

Jon-Ivar Skullerud<sup>a</sup>, Patrick O. Bowman<sup>b</sup> Ayşe Kızılersü<sup>c</sup>, Derek B. Leinweber<sup>c</sup>, Anthony G. Williams<sup>c</sup>

<sup>a</sup>School of Mathematics, Trinity College, Dublin 2, Ireland

<sup>b</sup>Nuclear Theory Center, Indiana University, Bloomington IN 47408, USA

<sup>c</sup>Centre for the Subatomic Structure of Matter, Adelaide University, Adelaide, SA 5005, Australia

We compute the quark–gluon vertex in quenched lattice QCD, in the Landau gauge using an off-shell mean-field  $\mathcal{O}(a)$ -improved fermion action. The complete vertex is computed in two specific kinematical limits, while the Dirac-vector part is computed for arbitrary kinematics. We find a nontrivial and rich tensor structure, including a substantial infrared enhancement of the interaction strength regardless of kinematics.

### 1. INTRODUCTION

Over the past few years, substantial progress has been made in our understanding of the non-perturbative correlation functions (propagators and vertices) of the fundamental fields of QCD and their relation to the phenomena of colour confinement and dynamical chiral symmetry breaking. It has recently become evident that at least in Landau gauge, a detailed knowledge of the structure of the quark–gluon vertex is essential for an understanding of the dynamics of quark confinement and chiral symmetry breaking, which is encoded in the quark Dyson–Schwinger equation (DSE), relating the quark propagator  $S(p)$  to the gluon propagator and the quark–gluon vertex  $\Gamma_\mu(p, q)$ , where  $p$  and  $q$  are quark and gluon momenta respectively.

The overall shape of the gluon propagator is now quite well known, both from lattice QCD [1,2] and from studies of the coupled ghost–gluon Dyson–Schwinger equations. It is now clear that if this is fed into the quark DSE together with a bare or QED-like vertex, the resulting quark propagator will not exhibit a sufficient degree of chiral symmetry breaking. Several of the contributions at this conference have addressed this issue, in various ways [3–6].

The quark–gluon vertex is related to the ghost

sector through the Slavnov–Taylor identity (STI),

$$q^\mu \Gamma_\mu(p, q) = G(q^2) \left[ (1 - B(q, p + q)) S^{-1}(p) - S^{-1}(p + q) (1 - B(q, p + q)) \right], \quad (1)$$

where  $G(q^2)$  is the ghost renormalisation function and  $B^a(q, k)$  is the ghost–quark scattering kernel. In particular, if the ghost propagator is infrared enhanced, as both lattice [7] and DSE studies [8] indicate, the vertex will also be so. This provides for a consistent picture of confinement and chiral symmetry breaking at the level of the Green’s functions of Landau-gauge QCD, where the same infrared enhancement that is responsible for confinement of gluons, provides the necessary interaction strength to give rise to dynamical chiral symmetry breaking in the quark sector.

Confinement of quarks is still not understood in this picture, however. If the effective interaction between a quark and an antiquark by way of exchange of a nonperturbative gluon is to give rise to a linearly confining potential, the quark–gluon vertex must contain an infrared enhancement over and above that contained in the ghost self-energy. In the STI, this would be encoded in a non-trivial ghost–quark scattering kernel. Confirming or refuting this picture is a major challenge for current lattice and DSE studies of Landau-gauge QCD.

Another area where the quark–gluon vertex may be of interest is that of effective charges. Al-

\*Talk presented by JIS

though ‘the running coupling’ is not a meaningful concept beyond perturbation theory, since there is no known way of nonperturbatively connecting two different ‘schemes’, process-dependent effective charges may be defined non-perturbatively and be phenomenologically useful. The interaction between quarks and gluons may be a natural starting point for many of the physically interesting processes.

Here we will present results of a lattice investigation into the quark–gluon vertex [9]. This consists of a determination of the full structure of the vertex at two particular kinematical points (the *soft gluon point* where the gluon has zero momentum, and the *quark reflection point* where the incoming and outgoing quark momenta are equal and opposite), as well as a determination of the dominant, vector part of the vertex in arbitrary kinematics.

## 2. FORMALISM

We denote the outgoing quark momentum  $p$  and the outgoing gluon momentum  $q$ . The incoming quark momentum is  $k = p + q$ . In the continuum, the quark–gluon vertex can be decomposed into four components  $L_i$  contributing to the Slavnov–Taylor identity and eight purely transverse components  $T_i$ :

$$\Gamma_\mu(p, q) = \sum_{i=1}^4 \lambda_i(p^2, q^2, k^2) L_{i,\mu}(p, q) + \sum_{i=1}^8 \tau_i(p^2, q^2, k^2) T_{i,\mu}(p, q). \quad (2)$$

In euclidean space, the components  $L_i$  and  $T_i$  are given by [9]

$$\begin{aligned} L_{1,\mu} &= \gamma_\mu & L_{2,\mu} &= -\not{P} P_\mu & (3) \\ L_{3,\mu} &= -i P_\mu & L_{4,\mu} &= -i \sigma_{\mu\nu} P_\nu \\ T_{1,\mu} &= -i \ell_\mu & T_{2,\mu} &= -\not{P} \ell_\mu \\ T_{3,\mu} &= \not{q} q_\mu - q^2 \gamma_\mu \\ T_{4,\mu} &= -i [q^2 \sigma_{\mu\nu} P_\nu + 2q_\mu \sigma_{\nu\lambda} p_\nu k_\lambda] \\ T_{5,\mu} &= -i \sigma_{\mu\nu} q_\nu & T_{6,\mu} &= (qP) \gamma_\mu - \not{q} P_\mu & (4) \\ T_{7,\mu} &= -\frac{i}{2} (qP) \sigma_{\mu\nu} P_\nu - i P_\mu \sigma_{\nu\lambda} p_\nu k_\lambda \\ T_{8,\mu} &= -\gamma_\mu \sigma_{\nu\lambda} p_\nu k_\lambda - \not{p} k_\mu + \not{k} p_\mu, \end{aligned}$$

where  $P_\mu \equiv p_\mu + k_\mu$ ,  $\ell_\mu \equiv (pq)k_\mu - (kq)p_\mu$ . In Landau gauge, for  $q \neq 0$ , we are only able to compute the transverse projection of the vertex,  $\Gamma_\mu^P(p, q) \equiv P_{\mu\nu}(q) \Gamma_\nu(p, q)$ , where  $P_{\mu\nu}(q) \equiv \delta_{\mu\nu} - q_\mu q_\nu / q^2$  is the transverse projector. Since the vertex will always be coupled to a gluon propagator which contains the same projector, this is also the only combination that appears in any application. The four functions  $L_{i,\mu}$  are projected onto the transverse  $T_{i,\mu}$ , giving rise to modified form factors

$$\begin{aligned} \lambda'_1 &= \lambda_1 - q^2 \tau_3; & \lambda'_2 &= \lambda_2 - \frac{q^2}{2} \tau_2; & (5) \\ \lambda'_3 &= \lambda_3 - \frac{q^2}{2} \tau_1; & \lambda'_4 &= \lambda_4 + q^2 \tau_4. \end{aligned}$$

The lattice tensor structure is more complex, and Eq. (2) is only recovered in the continuum. The form factors also receive large contributions from lattice artefacts at tree level; the procedure we apply in correcting for these is described in [10].

In QED, the four form factors  $\lambda_i$  are completely determined by the fermion propagator  $S^{-1}(p) = i \not{p} A(p^2) + B(p^2)$ :

$$\lambda_1(p^2, q^2, k^2) = \frac{1}{2} (A(p^2) + A(k^2)); \quad (6)$$

$$\lambda_2(p^2, q^2, k^2) = -\frac{1}{2} \frac{A(p^2) - A(k^2)}{p^2 - k^2}; \quad (7)$$

$$\lambda_3(p^2, q^2, k^2) = \frac{B(p^2) - B(k^2)}{p^2 - k^2}; \quad (8)$$

$$\lambda_4(p^2, q^2, k^2) = 0. \quad (9)$$

By comparing our results with these forms we can get an idea of the importance of the nonabelian contributions to the STI, and in particular the quark–ghost scattering kernel.

## 3. RESULTS

We have analysed 495 configurations on a  $16^3 \times 48$  lattice at  $\beta = 6.0$ , using a mean-field improved SW action with a quark mass  $m \approx 115$  MeV. This is part of the UKQCD data set described in [11]; further details can also be found in [9]. A second quark mass  $m \approx 60$  MeV has also been studied, but as the mass dependence was found to be almost negligible [10], we do not show those results here.

### 3.1. Soft gluon point $q = 0$

At  $q = 0$  the vertex reduces to

$$\Gamma_\mu(p, 0) = \lambda_1(p^2)\gamma_\mu - 4\lambda_2(p^2)\not{p}p_\mu - 2i\lambda_3(p^2)p_\mu, \quad (10)$$

where for brevity we write  $\lambda_i(p^2, 0, p^2) = \lambda_i(p^2)$ . In this specific kinematics, the QED expressions Eqs. (6)–(8) become<sup>2</sup>

$$\lambda_1^{\text{QED}}(p^2) = A(p^2); \quad (11)$$

$$\lambda_2^{\text{QED}}(p^2) = -\frac{1}{2}\frac{d}{dp^2}A(p^2); \quad (12)$$

$$\lambda_3^{\text{QED}}(p^2) = \frac{d}{dp^2}B(p^2). \quad (13)$$

In Fig. 1 we show the dimensionless quantities  $\lambda_1$ ,  $4p^2\lambda_2$  and  $2p\lambda_3$  as a function of momentum  $p$ . We also show the abelian forms Eqs. (11)–(13) which have been obtained from fitting lattice data for the quark propagator [10,12]. All these form factors have been renormalised at 2 GeV, requiring  $\lambda_1(4\text{ GeV}^2, 0, 4\text{ GeV}^2) = 1$ .

We find that while  $\lambda_3$  is quite close to its abelian form, both  $\lambda_1$  and  $\lambda_2$  are significantly enhanced. Since the ghost self-energy would contribute the same prefactor (in this kinematics, a constant) to all three form factors compared to the abelian form, this points to a nontrivial structure in the quark–ghost scattering kernel. However, the singular nature of the soft gluon point along with our small lattice volume make it difficult to draw firmer conclusions.

### 3.2. Quark reflection point $p = -k$

At the quark reflection point  $p = -k, q = -2p$  only  $\lambda'_1$  and  $\tau_5$  survive, and the projected vertex is

$$\Gamma_\mu^P(-q/2, q) = \lambda'_1(q^2)(\gamma_\mu - \not{q}q_\mu/q^2) - i\tau_5(q^2)\sigma_{\mu\nu}q_\nu, \quad (14)$$

where in this section we write  $\{\lambda'_1, \tau_5\}(q^2/4, q^2, q^2/4) = \{\lambda'_1, \tau_5\}(q^2)$ . The dimensionless quantities  $\lambda'_1(q^2), q\tau_5(q^2)$  are shown

<sup>2</sup>In [10] the expressions for  $\lambda_2$  and  $\lambda_3$  had the wrong sign. We are grateful to Craig Roberts for bringing these errors to our attention. In the same paper, the lattice data for  $\lambda_3$  and for  $\tau_5$  at the quark reflection point also had the wrong sign.

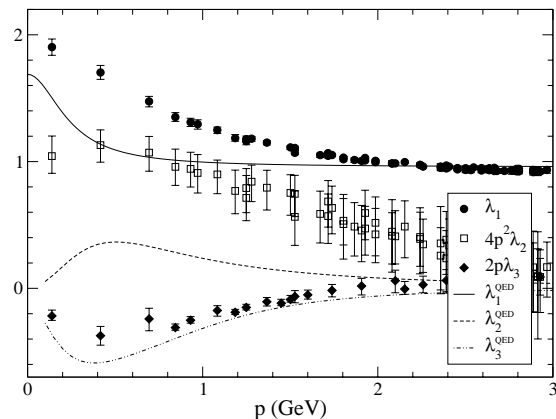


Figure 1. The renormalised, dimensionless form factors  $\lambda_1$ ,  $4p^2\lambda_2$  and  $2p\lambda_3$  at the soft gluon point, as a function of  $p$ , for  $m = 115$  MeV. Also shown are the corresponding abelian (Ball–Chiu) forms Eqs. (11)–(13), derived from the quark propagator.

in Fig. 2. These form factors have been renormalised requiring  $\lambda'_1(1\text{ GeV}^2, 4\text{ GeV}^2, 1\text{ GeV}^2) = 1$ .  $\lambda'_1$  shows the same qualitative behaviour as  $\lambda_1$  at the soft gluon point, with a quite strong infrared enhancement. We see that  $\tau_5$ , which has rarely if ever been included in vertex models used in DSE studies, is quite sizeable, indeed comparable in magnitude to the dominant component  $\lambda'_1$ . It will be interesting to study the effect of including this part of the vertex in future DSE studies.

### 3.3. General kinematics

The general lattice tensor structure, even for the Dirac-vector part of the vertex alone, is very complicated and makes a full determination of the vertex very difficult with this lattice action. However, in the special case where we choose both the quark and gluon momentum vectors to be ‘perpendicular’ to the vertex component, i.e. if we compute  $\Gamma_\mu(p, q)$  with  $p_\mu = q_\mu = 0$ , this structure simplifies considerably. There is no loss of generality provided rotational symmetry is restored in the continuum. Here, we will only study the leading, vector part of the vertex, but the other

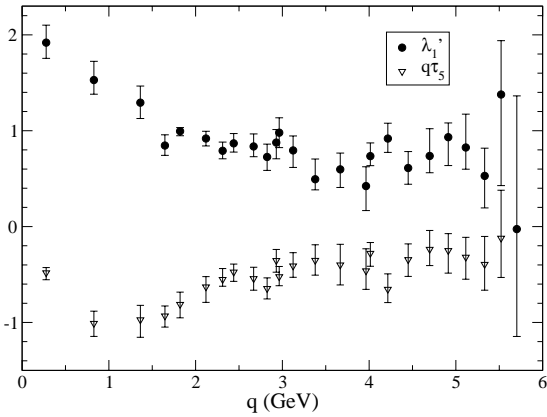


Figure 2. The renormalised, dimensionless form factors  $\lambda'_1$  and  $q\tau_5$  at the quark reflection point, as a function of the gluon momentum  $q$ , for  $m = 115$  MeV.

components may also be determined in principle. In continuum notation, we compute

$$\frac{1}{4} \text{tr} \gamma_\mu \Gamma_\mu^P(p, q) = \left(1 - \frac{q_\mu^2}{q^2}\right) \lambda'_1 + \frac{2}{q^2} [(pq)k_\mu - (kq)p_\mu] (p_\mu + k_\mu) \lambda'_2 \quad (15)$$

$$- [k^2 - p^2 - (k_\mu^2 - p_\mu^2)] \tau_6 = \lambda'_1 - (k^2 - p^2) \tau_6 \equiv \lambda'' \quad (16)$$

Of particular interest is the quark-symmetric limit, where the two quark momenta are equal in magnitude,  $p^2 = k^2$ . In this case,  $\tau_6$  is also eliminated, i.e.  $\lambda''(p^2, q^2, p^2) = \lambda'_1(p^2, q^2, p^2)$ . Note that both the soft gluon and the quark reflection kinematics discussed previously are specific instances of this more general case. The details of the lattice implementation of this, including the tree-level correction, will be described elsewhere [13]. In Fig. 3 we show  $\lambda'_1$  as a function of the two remaining independent momentum invariants. The data become quite noisy as  $q$  is increased, and also exhibit some ‘spikes’ and ‘troughs’ which at present we assume to be numerical noise and lattice artefacts.

By interpolating the points in Fig. 3, we may

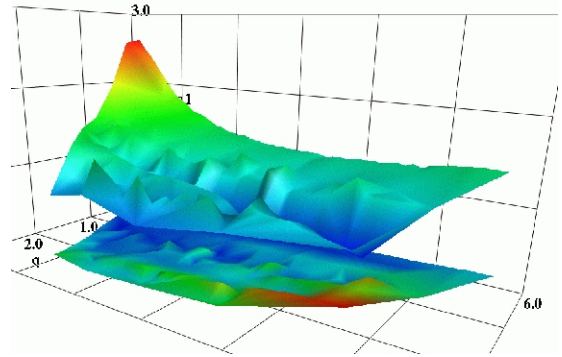


Figure 3. The unrenormalised form factor  $\lambda'_1$  in the quark-symmetric kinematics  $p^2 = k^2$  (upper surface), as a function of quark momentum  $p$  (long axis) and gluon momentum  $q$  (short axis) in units of GeV. Statistical uncertainties are illustrated by the lower surface.

reach the totally symmetric point where  $p^2 = k^2 = q^2$ . This kinematics has a history of being used to define a momentum subtraction (MOM) scheme [14]. We show our results in Fig. 4. Again we find a strong infrared enhancement.

Finally, Figs. 5 and 6 show  $\lambda''_1$  in general kinematics, for four different fixed values of  $q$ , as a function of the two quark momenta  $p$  and  $k$ . We expect all form factors to be symmetric in  $p^2$  and  $k^2$  ( $\tau_6$  on its own is antisymmetric, but is multiplied by  $p^2 - k^2$ ), and this is also what the figures show, within errors. The broadening of the data surface as  $q$  grows is simply a reflection of the increase in available phase space.

The same qualitative features as were found in the more specific kinematics, are reproduced here. At low  $q$ , we see a clear infrared enhancement, which disappears as  $q$  grows, reflecting the fact that at high momentum scales, only the logarithmic behaviour (which is too weak to be seen in these data) remains. At the same time, the level of the surface sinks, which reflects the infrared enhancement of  $\lambda''_1$  also as a function of gluon momentum.

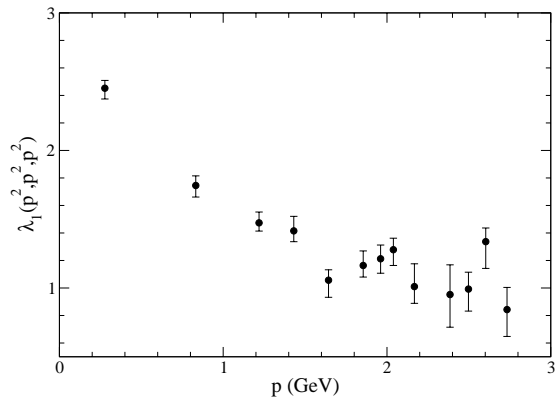


Figure 4. The unrenormalised form factor  $\lambda'_1$  at the totally symmetric kinematics  $p^2 = k^2 = q^2$ , as a function of the momentum  $p$ .

#### 4. DISCUSSION AND OUTLOOK

We have determined the complete tensor structure of the quark–gluon vertex at two kinematical points, as well as the leading component in arbitrary kinematics. At the soft gluon point, we have observed significant and non-uniform deviations from the abelian form which has previously been the basis for DSE studies. At the quark reflection point, we find a significant contribution from the ‘chromomagnetic’ form factor  $\tau_5$ , which has previously been ignored. In general kinematics, we find an infrared enhancement in all momentum directions; we hope to be able to quantify this enhancement more clearly by fitting the data in the infrared region to functional forms in the three momentum variables  $(p^2, k^2, q^2)$ .

It is interesting to compare these results with recent calculations based on nonperturbative extensions of the one-loop vertex [15,5]. Both these studies agree very well with our results for  $\lambda_1$  and  $\lambda_3$ , while finding substantially lower values for  $\lambda_2$ . Since all these calculations must be considered preliminary, too much emphasis should not be placed on this. It is worth noting that  $\lambda_2$  is inherently noisy, as it mixes with  $\lambda_1$ , which must be subtracted in order to obtain the data shown in Fig. 1.

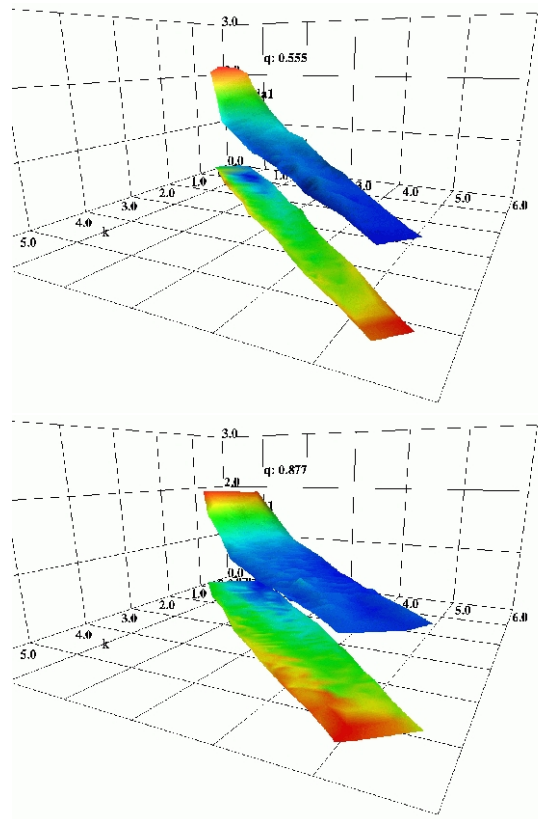


Figure 5. The unrenormalised form factor  $\lambda'_1$  for gluon momentum  $q = 0.555$  GeV (top) and  $q = 0.873$  GeV (bottom), as a function of quark momenta  $p$  and  $k$ . The lower surfaces denote the statistical uncertainties.

These results have been obtained on a rather small lattice, and with a discretisation that gives rise to quite large tree-level lattice artefacts which must be corrected for. We therefore expect systematic errors to be large for large momenta. To obtain more reliable results, and to extend this study to the full vertex structure at all kinematics, it would be desirable to employ an action which is known to have smaller and more tractable tree-level artefacts. The Asqtad action has been employed successfully in computing the quark propagator [16], and unlike the SW ac-

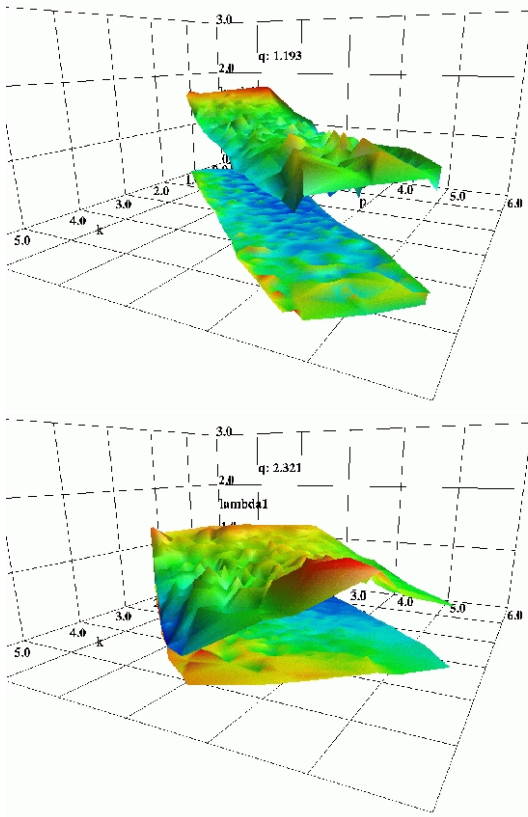


Figure 6. As Fig. 5, but for gluon momentum  $q = 1.193$  GeV and  $2.321$  GeV.

tion, only  $\lambda_1$  and possibly  $\lambda_2$  are non-zero at tree level, so tree-level correction will not be needed for the remaining form factors. This action is also computationally cheap, making large lattice volumes feasible. Another possibility is to use overlap fermions, which have the advantage of retaining an exact chiral symmetry, which protects all the odd Dirac components of the vertex at tree level.

## ACKNOWLEDGMENTS

This work has been supported by the Australian Research Council and the Irish Research Council for Science, Engineering and Technology.

JIS is grateful for the hospitality of the Centre for the Subatomic Structure of Matter, where part of this work was carried out. We thank Reinhard Alkofer, Christian Fischer and Craig Roberts for stimulating discussions.

## REFERENCES

1. F. D. R. Bonnet, P. O. Bowman, D. B. Leinweber, A. G. Williams and J. M. Zanotti, Phys. Rev. **D64** (2001)034501, [hep-lat/0101013].
2. P. O. Bowman, U. M. Heller, D. B. Leinweber, M. B. Parappilly and A. G. Williams, hep-lat/0402032.
3. A. Höll, A. Krassnigg and C. D. Roberts, nucl-th/0408015; M. S. Bhagwat, A. Höll, A. Krassnigg, C. D. Roberts and P. C. Tandy, nucl-th/0403012.
4. H. Iida, M. Oka and H. Suganuma, hep-ph/0312328; H. Iida, these proceedings.
5. C. S. Fischer, F. Llanes-Estrada and R. Alkofer, hep-ph/0407294.
6. P. C. Tandy, nucl-th/0408037.
7. J. C. R. Bloch, A. Cucchieri, K. Langfeld and T. Mendes, Nucl. Phys. **B687** (2004) 76, [hep-lat/0312036].
8. C. S. Fischer and R. Alkofer, Phys. Lett. **B536** (2002) 177, [hep-ph/0202202].
9. J. Skullerud and A. Kızılersü, JHEP **09** (2002) 013, [hep-ph/0205318].
10. J. I. Skullerud, P. O. Bowman, A. Kızılersü, D. B. Leinweber and A. G. Williams, JHEP **04** (2003) 047 [hep-ph/0303176].
11. UKQCD, K. C. Bowler *et al.*, Phys. Rev. **D62** (2000) 054506, [hep-lat/9910022].
12. P. O. Bowman, U. M. Heller, D. B. Leinweber and A. G. Williams, Nucl. Phys. Proc. Suppl. **119** (2003) 323, [hep-lat/0209129].
13. J.-I. Skullerud *et al.*, Quark-gluon vertex in general kinematics, in preparation.
14. W. Celmaster and R. J. Gonsalves, Phys. Rev. **D20** (1979) 1420.
15. M. S. Bhagwat and P. C. Tandy, hep-ph/0407163.
16. P. O. Bowman, U. M. Heller and A. G. Williams, Phys. Rev. **D66** (2002) 014505, [hep-lat/0203001].